

Soft x-ray laser ablation of metals and dielectrics

A. Faenov^{*1,2}, T. Pikuz^{2,3}, M. Ishino⁴, N. Inogamov⁵, V. Zhakhovsky⁶, I. Skobelev^{2,7}, N. Hasegawa⁴, M. Nishikino⁴, M. Kando⁴, R. Kodama^{1,3}, T. Kawachi⁴

¹Open and Transdisciplinary Research Initiative, Osaka University, Osaka 565-0871, Japan

²Joint Institute for High Temperatures, Russian Academy of Sciences, Moscow 125412, Russia

³Graduate School of Engineering, Osaka University, Osaka 565-0871, Japan

⁴Kansai Photon Science Institute, QST, Kizugawa, Kyoto 619-0215, Japan

⁵Landau Institute for Theoretical Physics, Russian Academy of Sciences, Chernogolovka 142432, Russia

⁶Dukhov All-Russia Research Institute of Automatics, Rosatom, Moscow, Russia

⁷National Research Nuclear University MEPhI - Moscow, 115409, Russia

ABSTRACT

We present an overview of our systematic studies of the surface modifications resulting from the interactions of both single and multiple picosecond soft x-ray laser (SXRL) pulses with materials, such as gold (Au), copper (Cu), aluminum (Al), and lithium fluoride (LiF). We show experimentally the possibility of the precise nanometer size structures (~10–40 nm) formation on their surfaces by ultra-low (~10–30 mJ/cm²) fluencies of single picosecond SXRL pulse. Comparison experimental results with the atomistic model of ablation, which was developed for the single SXRL shot interaction with dielectrics and metals, is provided. Theoretical description of surface nanostructures is considered and is shown that such structures are formed after laser illumination in a process of mechanical spallation of ultrathin surface layer of molten metal. Spallation is accompanied by a strong foaming of melt, breaking of foam, and freezing of foam remnants. Those remnants form chaotic nanostructures, which are observed in experiments. Our measurements show that electron temperature of matter under irradiation of SXRL was lower than 1 eV. The model calculation also predicts that the ablation induced by the SXRL can create the significant low electron temperature. Our results demonstrate that tensile stress created in LiF and metals by short SXRL pulse can produce spallative ablation of target even for drastically small fluencies, which open new opportunities for material nano processing.

Keywords: soft x-ray laser, surface modification, ablation threshold, modification threshold, surface machining, laser produced plasma, electron temperature

1. INTRODUCTION

Laser-matter interaction has a great fundamental interest and very important for realization of many industrial applications. Ablations by the long and short laser pulses differ qualitatively. The first –evaporation, boiling, and, at higher laser fluencies, moving matter caused by ablative pressure - created in hot plasma corona. It is opposite for short laser pulses when the release of pressurized layer is the main process. Figure 1 shows how dramatically the laser ablation thresholds changed for long and short duration laser pulses both for visible and X-ray lasers. For the relatively long (~20 ps) incident laser pulses, it was shown¹ that the damage of dielectrics involves the heating of conduction band electrons and transferring of electron energy to the lattice. Damage occurs if the deposited energy is sufficient to melt or boil the dielectrics. Decreasing the pulse duration of lasers having the photon energy of around 1 eV sharply diminishes the ablation threshold of dielectrics from ~20–40 J/cm² down to ~2 J/cm². Such diminution in threshold is connected with transition from the thermally dominated regime of long pulse laser to an ablative regime dominated by collisional and multiphoton ionization with production of large number of electrons of short pulse laser. For an enough short pulse duration, the laser energy is absorbed by the electrons much faster than it is transferred to the lattice. This initiates the electron avalanche resulting in damage of dielectrics.

It is necessary to stress that interaction of short laser pulses with matter has a particular interest not only due to essential reduction of laser ablation thresholds, but also due to a non-stationary behavior of involved processes and transfer materials into warm dense matter states.

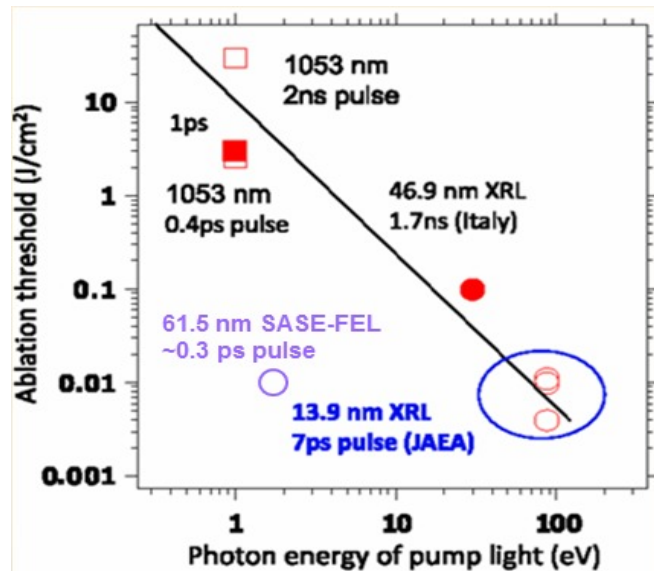


Figure 1. Comparison of the ablation thresholds (for incident fluence) for dielectrics as function of laser photon energy and laser pulse duration reported in Refs.^{2-4, 8, 19.}

Additionally there are many industrial applications using short pulse lasers. New exciting possibilities are appeared with the development of the X-ray lasers and particular X-ray lasers with picosecond or femtosecond pulse duration, which allowed applied them for ablation and nanostructured modification of different materials. In such case an even more efficient ablation of dielectrics could be reached by using extreme ultraviolet radiation or SXRL.

Here we present the overview of main results, which have been obtained in our recent investigations²⁻¹⁸ of SXRL interaction with metals and dielectrics.

EXPERIMENTAL RESULTS

Presented results (shown in Figs. 3–6) have been obtained at two different SXRL facilities - one is at the Kansai Photon Science Institute of National Institutes for Quantum and Radiological Science and Technology (QST) and the other is at RIKEN Spring-8 Center.

In first case, the SXRL pulse was generated from silver (Ag) plasma mediums, which were used in an oscillator-amplifier configuration with double targets¹⁹. The characteristics of the generated SXRL pulse from the Ag double targets were the following: wavelength of 13.9 nm (photon energy of 89 eV), bandwidth of narrower than 10^{-4} , and duration of 7 ps. The output energy varied with each shot, and the pulse-to-pulse fluctuation was evaluated to be 70–80% from 15 consecutive laser shots. However, the fluctuation of the nearest five shots was relatively small, i.e., less than 22%. The experimental set up is shown in Fig. 2. The SXRL pulse was focused on a sample surface by using a Mo/Si multilayer coated spherical mirror having a radius of curvature of 1000 mm. The Mo/Si multilayer coating was optimized for soft x-rays with a wavelength of 13.9 nm at an incidence angle of 2° , and it was placed approximately 2640 mm from the SXRL output. Then 0.2 μm thick Zr filters were placed in front of the spherical mirror in order to reduce the scattered optical radiations from the Ag plasmas.

As target materials, Al, Cu, Au plates and LiF crystal were used. These samples were mounted on a sample stage that had two movable directions. The sample was moved after the prescribed number of shots along the propagation direction of the incident SXRL beam around the best focal position, and it was also moved perpendicular to the propagation direction in order to be irradiated on a fresh surface. All target surfaces were well synchronized to ensure identical focusing conditions. The distribution of the formed features on each sample surface represents the distribution of the gain structures in the Ag plasmas, because the spherical mirror reconstructs a reduction image of the SXRL source. The SXRL irradiation of different targets was carried out in a vacuum chamber. Due to the transmittance of the Zr filter and the reflectivity of the Mo/Si mirror at a wavelength of 13.9 nm, which are were approximately 48% and 50% , the total energy of the SXRL pulse reaching the sample surface was approximately 48 nJ. At this wavelength with normal

incident irradiation, almost the entire incident energy of x-ray photons was absorbed by the samples. The SXRL pulse intensity profiles and stabilities were confirmed using a LiF detector. It was found that the SXRL energy concentration in

XRL source – Ag plasma

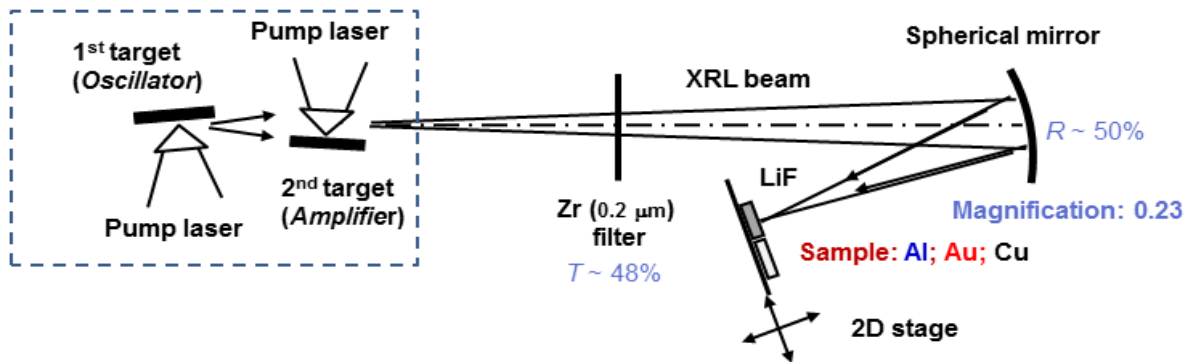


Figure 2. The experimental set up for recording the focusing SXRL beam on a LiF crystal and metal targets¹⁰.

the best focusing areas reached approximately 60%. Approximately 40% of the focusing SXRL energy was concentrated in the center of the best focusing spots⁷ as a result, the SXRL energy at the center of the best focal spot was ~12 nJ. Experiments with single shot irradiation of materials surfaces and multiple shot irradiations were performed.

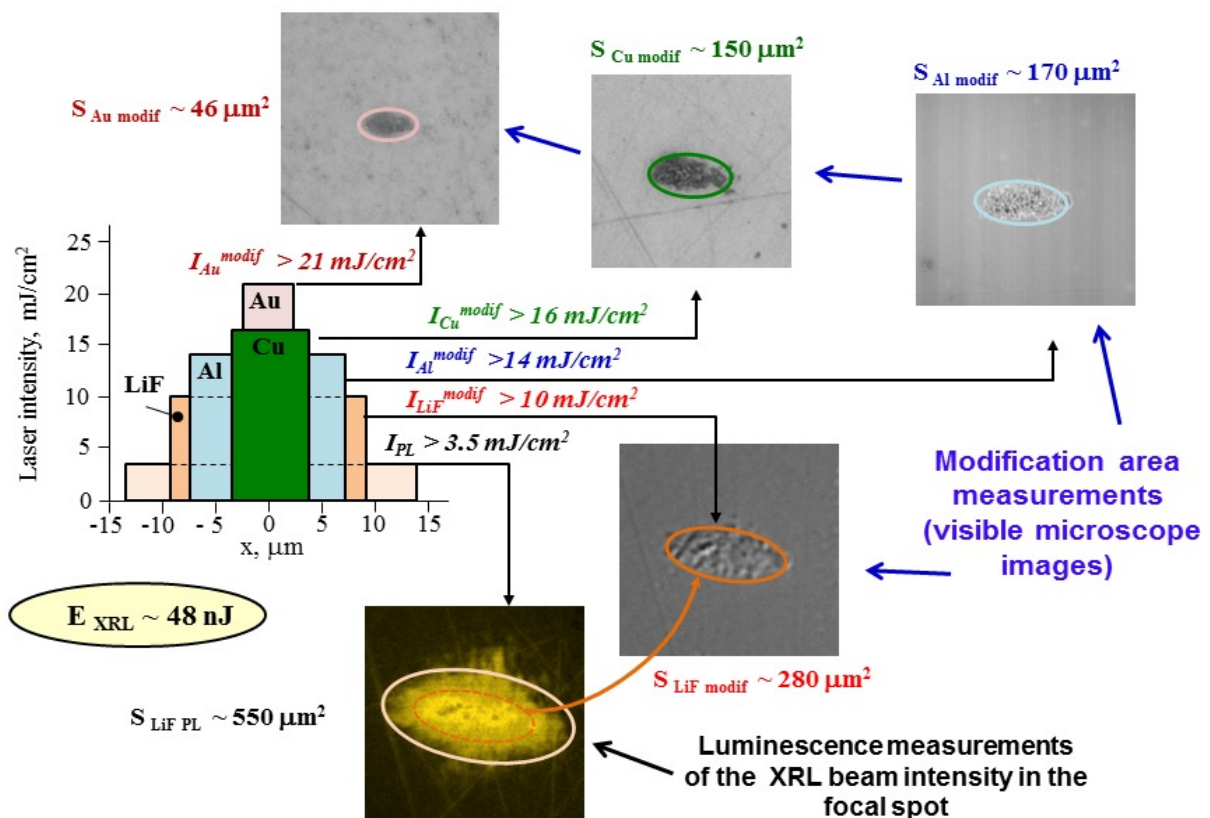


Figure 3. The luminescent image of LiF surface and microscope images of LiF, Al, Cu, and Au surfaces. SXRL fluences on target samples are estimated from averaged values in modification zone.

In the second case, SXRL pulse was provided with the self-amplified spontaneous emission-free electron laser (SASE-FEL) facility. The experiments were performed at the SPring-8 Compact SASE Source (SCSS)²⁰. This system provided laser in the extreme ultraviolet (EUV) region (51–62 nm). In our experiments, SCSS worked at wavelengths about 61.5 nm. A single shot mode was used, which allowed us to measure the laser energy in each shot. SCSS pulse energy was varied from 4 to 11 μJ in different shots. The duration of the pulse was about 300 fs. To find the ablation threshold of LiF crystals, the pulse energy and/or focusing size were changed. The beam size could be changed by the moving sample position along the beam axis. The luminescence of stable color centers (CCs) formed by EUV-FEL radiation²¹ was used to measure the intensity/fluence distribution in SCSS laser focal spots³. It allows to define an accurate value of the real local fluence at a target surface, and to find exact values of the ablation threshold. Due to strong aberrations, the intensity distribution has complicated smeared-out shape and, at near ablation threshold (F_{abl}) only, a small part (20–40%) of pulse energy is inside the ablation crater⁸.

In both type of experiments the photo-luminescence patterns from CCs in LiF (after irradiation of SXRL or EUV-FEL beams) were observed by using a confocal fluorescence laser microscope. To confirm that the surface conditions, a visible microscope with differential modes was used. To analyze the details of the induced structures, which could not be seen with an optical microscope, a scanning electron microscope (SEM) and an atomic force microscope (AFM) were also used.

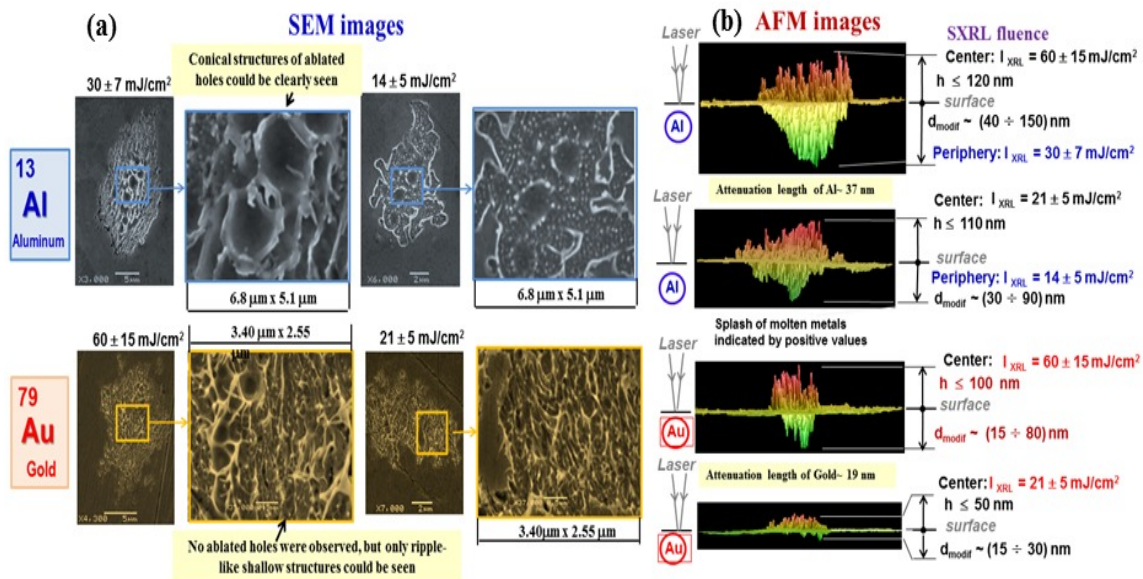


Figure 4. Single shot X-ray laser interaction with metals: surface modification has very different topology for Al and Au^{7,9,18}. (a) SEM images and (b) cross sectional profiles measured by AFM.

The main results obtained in both experiments with SXRL and SCSS beams are the following:

- 1) Strong lowering of ablation threshold of dielectrics in the case of its irradiation by picosecond SXRL pulses compare with nano- or sub- picosecond visible laser pulses or SXRL pulses with nanosecond duration have demonstrated (See Fig. 1). It was shown that SXRL fluence for 7 ps SXRL pulses and 300 fs SCSS pulses the nanostructure modification of LiF surfaces started from 10 mJ/cm^2 .
- 2) From the estimation of fluences in the ablation and modified parts that appear on the Al surfaces, it can be concluded that the nano- modification thresholds of surfaces are: for Al were approximately $> 14 \text{ mJ/cm}^2$, for Au $> 21 \text{ mJ/cm}^2$, and for Cu $> 16 \text{ mJ/cm}^2$, respectively (See Fig. 3).
- 3) Conical structures were formed on the Al surface, whereas ripple-like structures were created on the Au and Cu surfaces irradiated by single SXRL pulse.
- 4) In the case of Au targets, no ablated holes were observed for any number of shots, but only slightly growth in depth modification could be seen (shown in Figs. 4–6). The structure has been changed from ripple-like shallow (single

shot), to “nanobranches” structure (after 2 shots) and to “spherical nanoparticles” (after 5 shots). In the case of Al targets, surface modification has completely different topology for single and multiple SXRL shots irradiation. Conical structures and ablated holes could be clearly seen for single irradiation, which with increasing of number of shots changed to “nanobranches” structures.

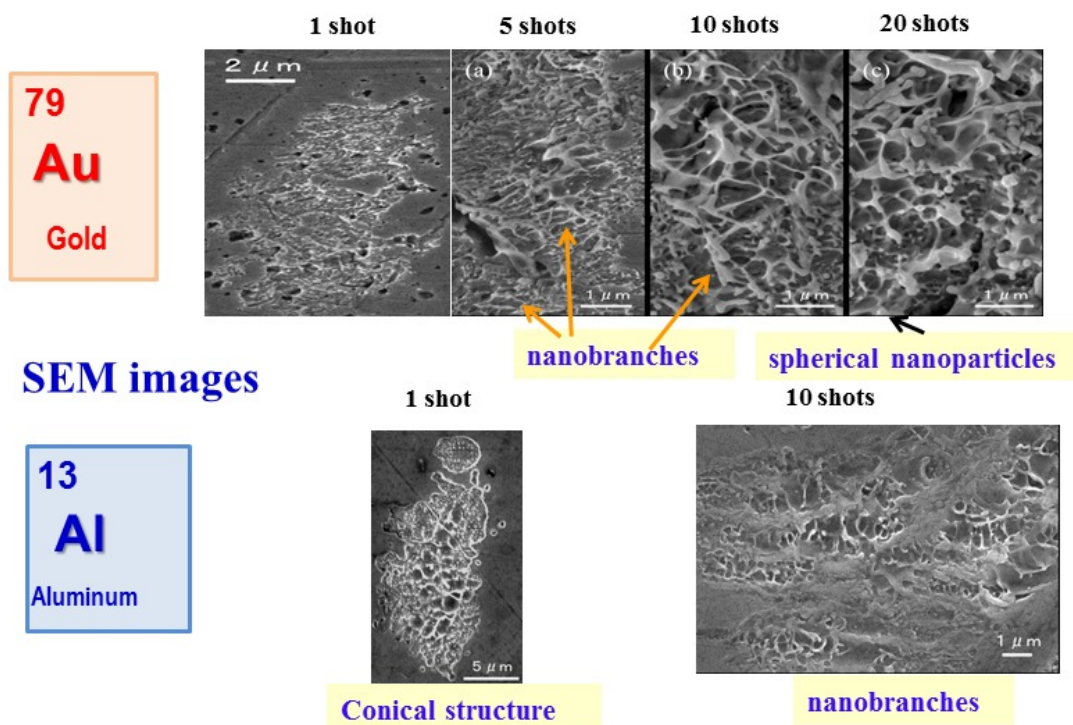


Figure 5. Multiple shots X-ray laser interaction with metals: surface modification has different topology for single and multiple shots for aluminum and gold targets¹¹.

- 5) Our investigation of the interactions of the SXRL beam with metals (Cu and Au) shows that nanometer size surface modification first occurs randomly at highly localized nanoscale sites. Based on the results of morphology and cross-sectional depth studies using SEM and AFM, we believe that these nanostructures are formed owing to the flow dynamics of a relocates materials from the center of the melted site to the peripheral area leading to the formation of nanoscale cavities, nanoscale rims, or nanoscale protrusions.
- 6) In addition, our results imply that the ablation and/or surface modification by the SXRL is not accompanied by plasma formation but is induced by thermo-mechanical pressure, which is so called a spallative ablation. This spallative ablation process occurs in the low electron temperature region (0.4–0.7 eV) of a non-equilibrium state of warm dense matter. Details are shown in Ref. 12.

3. SXRL BEAM INTERACTION WITH METALS AND DIELECTRICS

Main difference of infrared (IR) or visible laser, and SXRL interaction with matter is difference in energy of photons. Visible lasers has energy of photons in the order of energy of valence band and the following processes are important to consider for correct treatment of visible laser interaction with matter: multi-photon ionization, tunnel ionization, electron impact and avalanche influences. At the same time the SXRL quanta ionizes the internal shells. X-ray photons knock out electrons from deep levels and then make holes in the internal shells. Appearance of such deep holes triggers the Auger processes, while appearance of energetic electrons starts impact ionization. This causes the main difference with IR and visible photon absorption. In the case of SXRL laser interaction with matter impact ionization starts immediately with the heating by SXRL pulse. It is not necessary to wait when ionized

electrons accumulate enough energy by inverse bremsstrahlung to overcome the gap between valence and conduction bands. In the case of SXRL photons irradiation

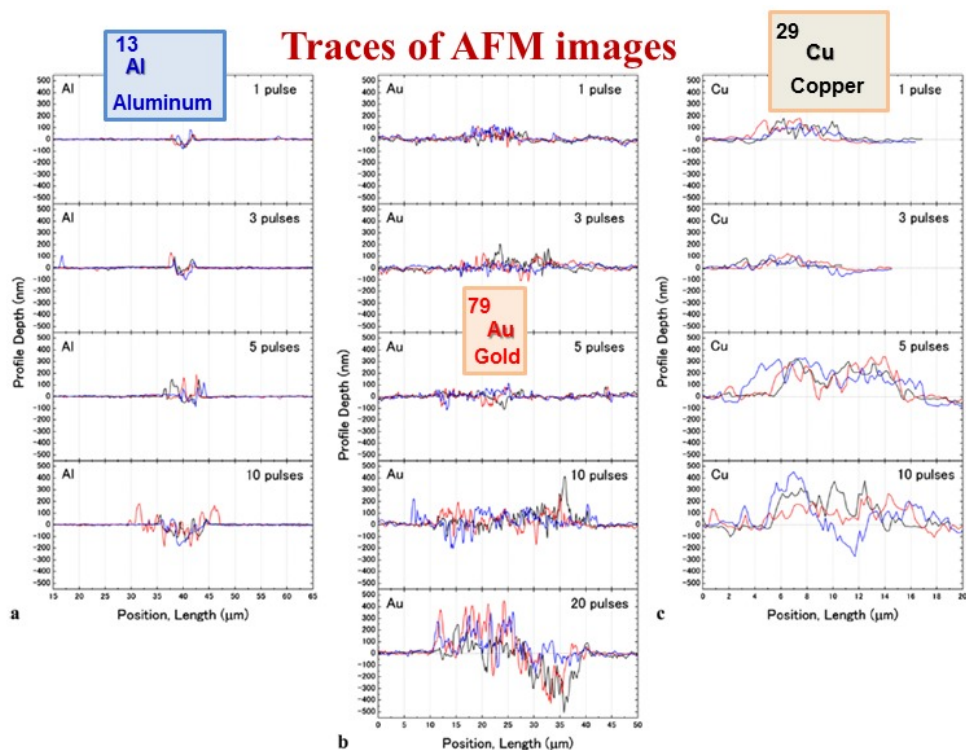


Figure 6. Comparison of single and multiple shots X-ray laser interaction with metals¹¹. Developments of the depth profiles for the (a) Al, (b) Au, and (c) Cu surface structures. The profiles shown in each figure are derived from the three lines that cross each modified area on the targets.

their attenuation depth varies in a wide range with energy of photons and Z-number of irradiated material. The attenuation depth for photon energy of the Ag X-ray laser (89 eV) is, for example, ~28 nm for LiF, ~37 nm for Al, ~40 nm for Cu, and ~19 nm for Au. The attenuation depth for photon energy of the SCSS beam (~21 eV) for LiF is of 18 nm. It is also necessary to remember that SXRL beam under normal incidence to the target is completely absorbed by matter, while for visible laser photons absorption usually is in the order of only 10–15 %.

Theoretical consideration of SXRL beams interaction with matter was done in Refs.^{4–6, 8, 9, 13–18}. In dielectrics, as well as in metals, a laser pulse is absorbed by electronic subsystem of condensed matter and its electron temperature increases. It causes the increasing of pressure (see Fig. 7). Meanwhile temperature of ionic subsystem (T_i)—increases more lately during the absorption and during the two-temperature (2T) stages. Duration of the laser pulse of Ag x-ray laser is $t_L = 7$ ps, duration the electron-ion energy exchange time t_{eq} of the 2T stage is few picoseconds. Therefore after few ps $T_i(x,t)$ profile tends to the established profile. The pressure profile decays into two acoustic waves: one of them (right) propagating into the bulk of a target, while the second wave (left) propagates toward the target boundary with vacuum. This is well known from 1-D solution of the wave equation, which is usually used to model of femtosecond visible laser light interaction with matter. The second wave reflects from the boundary and create the third (Reflected) acoustic wave. Interplay between these three (r, l, R) acoustic waves defines motion of target material (r = right, l = left, R = Reflected). The Reflected wave has a pressure amplitude opposite to the amplitude of the left wave, because reflection from a vacuum boundary changes sign of a wave: therefore a compression wave ($p > 0$) going to the left gradually transforms to a tensile wave ($p < 0$). If amplitude of a tensile wave overcomes strength of material then fragmentation begins and a part of a target breaks out from a rest of a target. Such a way of material removal from a target surface is called a thermo-mechanical ablation^{4–6, 8, 13, 14, 16, 17}. Modeling^{4–6, 8} shows that Ni-like Ag X-ray laser fluence of ~10 mJ/cm² is enough for removal of ~50 nm thick layer of LiF, which is in a very good coincidence with experimental data.

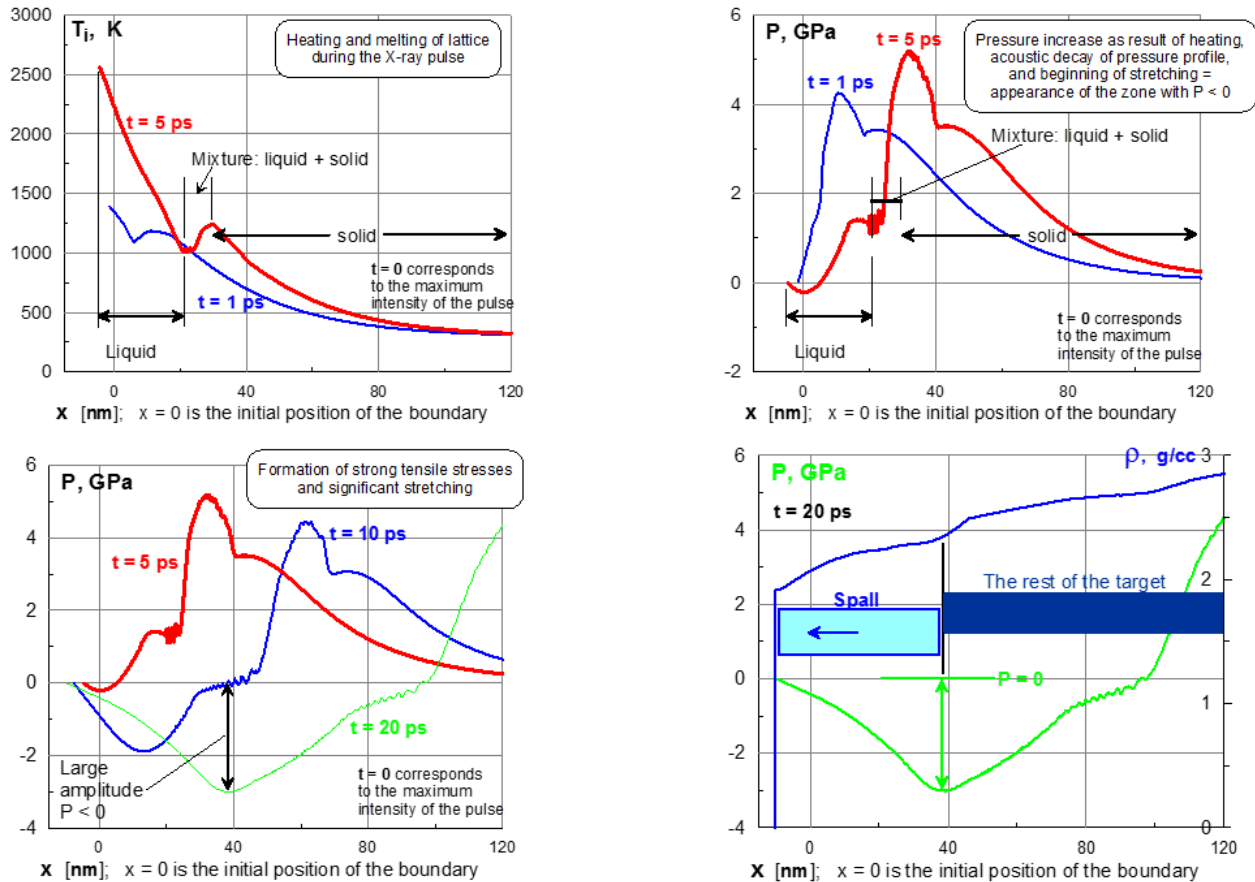


Figure 7. Photo-thermal mechanical modeling^{4-6,8} of SXRL interaction with dielectrics (LiF crystal). Modeling includes: absorption of X-ray photons and caused by them ionization of dielectric; Thermalization of electron subsystem; Two-temperature equations describing electron-ion temperature relaxation and hydrodynamic motion; Thermodynamic properties of LiF crystal.

Very important findings^{9, 13-15, 17, 18} of theoretical modeling of SXRL interaction with matter are demonstration that electron temperature and pressure dominate at an early two-temperature stage, which are causing lowering of nanostructure and ablation thresholds values. The modeling of nanostructures formation process on the surface of Aluminum is presented in Fig. 8. Such modeling was provided in Ref. 8 for absorbed fluence 80 mJ/cm^2 . Simulations shown in Figs. 8 is important for understanding of phenomena leading to appearance of chaotic structures. The key processes is foam stretching and breaking in interplay with freezing of super-cooled liquid. Hydrodynamic motions under action of inertia, tensile stress, and surface tension compete with an equally slow solidification up to the end of motion. A droplet at tip of jet demonstrates an amazing dynamics. Membranes surrounding bubbles in foam are ultimately stretched by inertial expansion up to 2-3 interatomic distances. Membranes break in their thinnest parts. This breaking forms a wall type feature made from a remnant of a membrane. The feature is topped with a droplet at its upper edge. The droplet is a formation elongated along the edge of membrane. It accumulates mass during contraction of broken membrane. It accumulates not only mass but also momentum of this mass. This momentum is created during contraction. Therefore velocity of a droplet differs from velocity of membrane itself. Complicated velocity field appears under action of surface tension and freezing/melting processes taking place in a contact between the liquid droplet and colder solidified membrane. The last picture in the series shown in Fig. 8 shows instant coexistence of liquid red droplet and frozen green jet type membrane. Experimental pictures in Figs. 4-6 present plenty examples of such membranes, jets, and droplets.

Theoretical considerations provided in Refs. 9, 15, 18 show that, at low laser pulse energy, the nanoscale ripples on the surface may be induced by melting without following ablation. In that case, the nanoscale changes in the surface are caused by splash of molten metal under gradient of fluence. At higher laser pulse energy, the ablation process occurs and

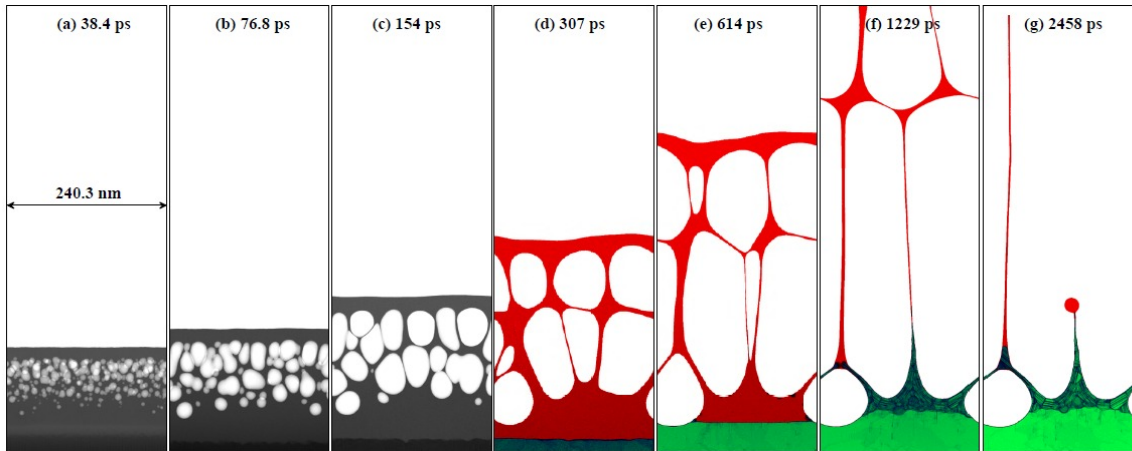


Figure 8. Nucleation, foaming, hydrodynamic decay of strongly stretched foam, appearance of droplets on the tip of jets, and freezing of remnants of broken liquid-vapor foam. Process covers two orders of magnitude in time. MD simulation spans scales from interatomic and up to micron size. Recrystallization front is clearly seen. It gradually approaches the foam region. Three first pictures present density maps. While the four next pictures show evolution of phase composition. The red and green colors correspond to liquid and solid aluminum, respectively. Dark green color correspond to a region with ultra-dense concentration of dislocations. This region forms a “skin” including the frozen surface nanostructures.

craters are formed on the surface. However, the melting determines the size of the modified surface at all ranges of the laser energies. The atomistic simulations of melting and ablation processes provided in Refs.^{15, 18} for Al and Au targets demonstrate the very good coincidence between the calculated threshold fluencies for melting and ablation with measured ones (see Fig. 9).

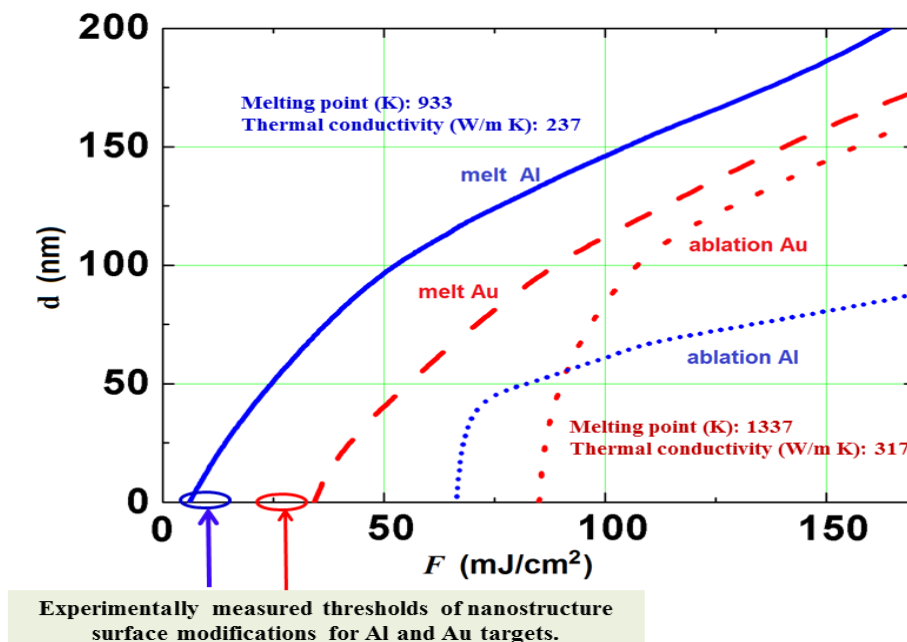


Figure 9. Comparison¹⁵ of experimental and modeled the melting and ablation depth dependences for SXRL irradiations of Au and Al targets. Good coincidence of nanostructure formation thresholds between theory and experiment is obviously seen

4. CONCLUSION

Our recent systematic experimental and theoretical investigations of SXRL and SCSS interaction with metals and dielectrics show that a short pulse of x-ray lasers causes a thermomechanical response and the appearance of tensile stress which overcomes material strength above ablation threshold. As a result spallative ablation is happened, while near threshold stretching of molten layer may be accompanied by nanostructuring.

The value of the X-ray threshold is small in comparison with irradiation by longer wavelengths and/or longer pulse. Our studies under a wide variety of experimental conditions shows that the optimal conditions for the formation of pure nanometer size structures can be achieved with only single pulse irradiation on the target material using an SXRL beam with very low fluence. Our results provide new input for the machining the surfaces of these materials. The wavelength of the SXRL is shorter than those of a visible or infrared laser, which in principle allowed that an SXRL potentially has the ability to draw small patterns. The modified surfaces had an average depth approximately several tens of nanometers. Hence, the SXRL could be considered as a future tool to fabricate nanometer scale three dimensional structures.

ACKNOWLEDGEMENTS

This work was supported by Grant-in-aid for Scientific Research (C) under Grants No. 16K05030, 16K04989, 17K05729 from JSPS, Japan. V. Z., N. I., T. P., and A. F. acknowledge support from Russian Science Foundation (14-19-01599).

REFERENCES

- [1] B. C. Stuart, M. D. Feit, S. Herman, A. M. Rubenchik, B. W. Shore, and M. D. Perry, “Nanosecond-to-femtosecond laser-induced breakdown in dielectrics”, *Phys. Rev. B* **53**, 1749 (1996).
- [2] A. Ritucci, G. Tomassetti, A. Reale, L. Arrizza, P. Zuppella, L. Reale, L. Palladino, F. Flora, F. Bongfigli, A. Faenov, T. Pikuz, J. Kaiser, J. Nilsen, A.F. Jankowski, “Damage and ablation of large bandgap dielectrics induced by a 46.9 nm laser beam”, *Optic Letters*, **31**, 68-71 (2006).
- [3] A.Ya. Faenov, N.A. Inogamov, V.V. Zhakhovskii, V.A. Khokhlov, K. Nishihara, Y. Kato, M. Tanaka, T.A. Pikuz, M. Kishimoto, M. Ishino, M. Nishikino, T. Nakamura, Y. Fukuda, S.V. Bulanov, T. Kawachi, “Low-threshold ablation of dielectrics irradiated by picosecond soft X-ray laser pulses”, *Applied Phys. Lett.* **94**, 231107 (2009).
- [4] N.A. Inogamov, A.Ya. Faenov, V.A. Khokhlov, V.V. Zhakhovskii, Yu.V. Petrov, I.Yu. Skobelev, K. Nishihara, Y. Kato, M. Tanaka, T.A. Pikuz, M. Kishimoto, M. Ishino, Y. Fukuda, S.V. Bulanov, T. Kawachi, “Spallative ablation of metals and dielectrics”, *Contributions to Plasma Physics Journal*. **49**, 455 – 466 (2009).
- [5] N.A. Inogamov · V.V. Zhakhovsky · A.Y. Faenov · V.A. Khokhlov · V.V. Shepelev · I.Y. Skobelev · Y. Kato · M. Tanaka · T.A. Pikuz · M. Kishimoto · M. Ishino · M. Nishikino · Y. Fukuda · S.V. Bulanov · T. Kawachi · Y.V. Petrov · S.I. Anisimov · V.E. Fortov, “Spallative ablation of dielectrics by X-ray laser”, *Appl Phys A. V.* **101**, 87-96 (2010).
- [6] N. A. Inogamov, A.Ya. Faenov, V.V. Zhakhovskii, I.Yu. Skobelev, V. A. Khokhlov, Y. Kato, M. Tanaka, T. A. Pikuz, M. Kishimoto, M. Ishino, M. Nishikino, Y. Fukuda, S.V. Bulanov, T. Kawachi, Yu.V. Petrov, S. I. Anisimov, V. E. Fortov, «Interaction of Short Laser Pulses in Wavelength Range from Infrared to X-ray with Metals, Semiconductors, and Dielectrics”, *Contrib. Plasma Phys.*, **51**, 361-366 (2011).
- [7] M. Ishino, A. Ya. Faenov, M. Tanaka, N. Hasegawa, M. Nishikino, S. Tamotsu, T. A. Pikuz, N. A. Inogamov, V. V. Zhakhovsky, I. Yu. Skobelev, V.E. Fortov, V.A. Khokhlov, V.V. Shepelev, T. Ohba, T. Kaihori, Y. Ochi, T. Imazono, «Nanoscale surface modifications and formation of conical structures at aluminum surface induced by single shot exposure of soft x-ray laser pulse”, *Journal of Applied Physics* **109**, 013504 (2011).
- [8] N. A. Inogamov, A. Ya. Faenov, V. V. Zhakhovsky, T. A. Pikuz, I. Yu. Skobelev, Yu. V. Petrov, V. A. Khokhlov, V. V. Shepelev, S. I. Anisimov, V. E. Fortov, Y. Fukuda, M. Kando, T. Kawachi, M. Nagasono, H. Ohashi, M. Yabashi, K. Tono, Y. Senda, T. Togashi, T. Ishikawa, “Two-Temperature Warm Dense Matter Produced by Ultrashort Extreme Vacuum Ultraviolet-Free Electron Laser (EUV-FEL) Pulse”, *Contrib. Plasma Phys.* **51**, 419 – 426 (2011).

- [9] S. V. Starikov, V. V. Stegailov, G. E. Norman, V. E. Fortov, M. Ishino, M. Tanaka, N. Hasegawa, M. Nishikino, T. Ohba, T. Kaihori, E. Ochi, T. Imazono, T. Kawachi, S. Tamotsu, T. A. Pikuz, I. Yu. Skobelev, A. Ya. Faenov. Laser ablation of Gold: Experiment and Atomistic simulation. *JETP Letters*, **93**, 642-647 (2011)
- [10] M. Ishino, A. Ya. Faenov, M. Tanaka, N. Hasegawa, M. Nishikino, S. Tamotsu, T.A. Pikuz, T. Ohba, T. Kaihori, and T. Kawachi, « Surface modifications of metals induced by soft x-ray laser pulse irradiations», *Journal of Laser Micro/Nanoengineering* **7**, 147 -151 (2012).
- [11] M. Ishino, A. Y. Faenov, M. Tanaka, S. Tamotsu, N. Hasegawa, M. Nishikino, T.A. Pikuz, T. Kaihori, T. Kawachi, « Observations of surface modifications induced by the multiple pulse irradiation using a soft picosecond x-ray laser beam», *Appl. Phys. A*. **110**, 179-188 (2013).
- [12] M. Ishino, N. Hasegawa, M. Nishikino, T. Pikuz, I. Skobelev, A. Faenov, N. Inogamov, T. Kawachi, M. Yamagiwa “Very low electron temperature in warm dense matter formed by focused picosecond soft x-ray laser pulses”, *Journal of Applied Physics* **116**, 183302 (2014).
- [13] N. A. Inogamov, V.V. Zhakhovskiy, S.I. Ashitkov, Y.N. Emirov, A.Y. Faenov, T.A. Pikuz, M. Ishino, M. Kando, N. Hasegawa, M. Nishikino, T. Kawachi, M.B. Agranat, A.V. Andriash, S. E. Kuratov and I.I. Oleynik, “Surface nano-structuring produced by spallation of metal irradiated by an ultrashort laser pulse”, *Journal of Physics: Conference Series* **500**, 112070 (2014).
- [14] N. A. Inogamov; V.V. Zhakhovskiy; V.A. Khokhlov; S.I. Ashitkov; Y.N. Emirov; K.V. Khichshenko; A.Ya. Faenov, T.A. Pikuz; M. Ishino; M. Kando; N. Hasegawa; M. Nishikino; P. S. Komarov; B.J. Demaske; M.B. Agranat; S.I. Anisimov; T. Kawachi; I.I. Oleynik, “Ultrafast lasers and solids in highly excited states: results of hydrodynamics and molecular dynamics simulations”, *Journal of Physics: Conference Series* **510**, 012041 (2014).
- [15] S. V. Starikov, A. Ya. Faenov, T. A. Pikuz, I. Yu. Skobelev, V. E. Fortov, S. Tamotsu, M. Ishino, M. Tanaka, N. Hasegawa, M. Nishikino, T. Kaihori, T. Imazono, M. Kando, T. Kawachi, “Soft picosecond X-ray laser nanomodification of gold and aluminum surfaces”, *Appl. Phys. B* **116**:1005–1016 (2014).
- [16] N. A. Inogamov, V. V. Zhakhovskiy, N. Hasegawa, M. Nishikino, M. Yamagiwa, M. Ishino, M. B. Agranat, S. I. Ashitkov, A. Ya. Faenov, V. A. Khokhlov, D. K. Ilnitsky, Yu. V. Petrov, K. P. Migdal, T. A. Pikuz, S. Takayoshi, T. Eyama, N. Kakimoto, T. Tomita, M. Baba, Y. Minami, T. Suemoto, T. Kawachi, “Hydrodynamics driven by ultrashort laser pulse: simulations and the optical pump — X-ray probe experiment”, *Appl. Phys. B* **119**, 413–419 (2015).
- [17] N.A. Inogamov, V.V. Zhakhovskiy, S.I. Ashitkov, Yu.N. Emirov, A.Ya. Faenov, Yu.V. Petrov, V.A. Khokhlov, M. Ishino, B.J. Demaske, M. Tanaka, N. Hasegawa, M. Nishikino, S. Tamotsu, T.A. Pikuz, I.Y. Skobelev, T. Ohba, T. Kaihori, Y. Ochi, T. Imazono, Y. Fukuda, M. Kando, Y. Kato, T. Kawachi, S.I. Anisimov, M.B. Agranat, I.I. Oleynik, V.E. Fortov, “Surface nanodeformations caused by ultrashort laser pulse”, *Engineering Failure Analysis* **47**, 328–337 (2015).
- [18] G. Norman, S. Starikov, V. Stegailov, V. Fortov, I. Skobelev, T. Pikuz, A. Faenov, M. Ishino, M. Tanaka, N. Hasegawa, M. Nishikino, S. Tamotsu, Y. Kato, T. Ohba, T. Kaihori, Y. Ochi, T. Imazono, Y. Fukuda, M. Kando, T. Kawachi, « Nanomodification of gold surface by picosecond soft X-ray laser pulse”, *Journ. Appl. Physics* **112**, 013104 (2012).
- [19] M. Tanaka, M. Nishikino, T. Kawachi, N. Hasegawa, M. Kado, M. Kishimoto, K. Nagashima, and Y. Kato, “X-ray laser beam with diffraction-limited divergence generated with two gain media”, *Opt. Lett.* **28**, 1680–1682 (2003).
- [20] T. Inagaki, S. Imoue, M. Ishi, Y. Kim, H. Kimura, M. Kitamura, T. Kobayashi, H. Maesaka, T. Masuda, S. Matsui, T. Matsushita, X. Marechal, M. Nagasono, H. Ohashi, T. Ohata, T. Ohshima, K. Onoe, K. Shirasawa, T. Takagi, S. Takahashi, M. Takeuchi, K. Tamasaku, R. Tanaka, Y. Tanaka, T. Tanikawa, T. Togashi, S. Wu, A. Yamashita, K. Yanagida, C. Zhang, H. Kitamura, and T. Ishikawa, “A compact free-electron laser for generating coherent radiation in the extreme ultraviolet region”, *Nature Photonics* **2**, 555 (2008).
- [21] G. Baldacchini, S. Bollanti, F. Bonfigli, F. Flora, P. Di Lazzaro, A. Lai, T. Marolo, R. M. Montecchi, D. Murra, A. Faenov, T. Pikuz, E. Nichelatti, G. Tomassetti, A. Reale, L. Reale, A. Ritucci, T. Limongi, L. Palladino, M. Francucci, S. Martellucci, and G. Petrocelli, “Soft X-ray submicron imaging detector based on point defects in LiF”, *Rev. Sci. Instrum.* **76**, 113104 (2005).